JOURNAL OF SPACECRAFT AND ROCKETS
Vol. 37, No. 4, July–August 2000

Interplanetary Flyby Mission Optimization Using a Hybrid Global–Local Search Method

Timothy Crain,* Robert H. Bishop,† and Wallace Fowler‡
University of Texas at Austin, Austin, Texas 78759-5321
and
Kenneth Rock§
Motorola, Leesburg, Virginia 20176

A hybrid optimization approach has been developed combining the global search properties of genetic algorithms with the local search characteristics of recursive quadratic programming. The genetic algorithm initially surveys the parameter space for candidate planetary encounter and maneuver occurrence times. The best candidate of the genetic algorithm parameter population is submitted as an initial parameter set to the recursive quadratic programming module for refinement. This hybrid optimizer was applied to ballistic Earth–Venus–Earth (EVE) and Earth–Mars–Earth (EME) flybys to minimize weighted mission ΔV constrained by Earth return energy and mission time of flight inequalities. These mission classes were chosen for their potential to demonstrate Mars transportation vehicle technology. Initial experiments with a time of flight limit of 480 days and an Earth-return energy limit of 14 km/s provided EME and EVE solutions with negligible ΔV at the respective flyby encounters. The hybrid optimizer required two orders of magnitude fewer trajectory evaluations to produce results equivalent to a grid search for this mission. The hybrid optimizer results indicate that a human Venus flyby transportation verification mission is superior to a Mars flyby mission.

Nomenclature

$\boldsymbol{C}$	= vector of constraint values
c	= rocket exhaust velocity, km/s
J	= scalar performance index
$\boldsymbol{O}(\boldsymbol{T})$	= vector of mission performance criteria evaluated at $\boldsymbol{T}$
$\boldsymbol{T}$	= set of optimization parameters defining planetary encounter times
t_{0-1}	= time offset from 1 January epoch to Earth departure, day
t_{1-2}	= time offset from Earth departure to Venus or Mars encounter, day
t_{1-3}	= time offset from Earth departure to Earth return, day
$V_{\infty,3}$	= hyperbolic excess velocity at Earth return, km/s
ΔV	= impulsive change in velocity, km/s
ΔV_{PFM}	= powered flyby maneuver impulse at Venus or Mars, km/s
ΔV_{TPI}	= transplanetary impulse required at Earth departure, km/s
δ_{Mars}	= trajectory turning angle relative to Mars at Mars flyby, deg
δ_{sun}	= trajectory turning angle relative to sun at planetary flyby, deg
δ_{Venus}	= trajectory turning angle relative to Venus at Venus flyby, deg
$\Theta_{\mathrm{mission}}$	= vector of operational constraints used by multiple-body gravity-assist trajectory tool
$\phi(\boldsymbol{T})$	= performance function

Introduction

GRAVITY-ASSIST trajectories make the most of interplanetary missions by reducing launch energies, thereby maximizing scientific and engineering payload mass fractions. Flyby missions of Venus have long been considered as a way to provide more payload delivery opportunities to Mars.[1–4] Indeed, missions such as Galileo[5] would be economically infeasible, or at least extremely limited in terms of scientific payload, if not for multiple gravity-assist flybys. A mission designer's challenge is to determine when the trajectory performance can be improved by employing gravity-assist flybys. The unavailability, complexity, and cost of gravity assist optimization programs for educational use prompted the creation of a program capable of optimizing multiple gravity-assist trajectories accurately and efficiently. The hybrid optimization program was formed by integrating the genetic algorithm[6] (GA) and the recursive-quadratic-program- (RQP-) based multiple-body gravity-assist trajectory tool (MGRAV) developed by Rock.[7] The GA and RQP codes existed as standalone optimizers that have independently been used to design interplanetary trajectories and to tune Kalman filters in adaptive navigation research. The hybrid optimizer is intended to be used as a preliminary design tool to help estimate mission cost and feasibility in terms of trajectory performance. This information can subsequently be used to estimate launch vehicle and propulsion system requirements, as well as provide preliminary information for thermal, power, and lifespan design considerations. To demonstrate this tool's applicability, prospective Earth–Mars–Earth (EME) and Earth–Venus–Earth (EVE) trajectories have been optimized for the period beginning 1 January 2002 and ending 31 December 2011. These trajectories are of interest as possible missions for the crewed Mars transportation and habitation vehicle TransHab. Following the lead of the Apollo lunar flyby missions that predated Apollo 11, a Venus or Mars flyby trajectory would serve to verify the ability of the TransHab to sustain astronauts in the interplanetary environment without the additional complexity of a Mars entry and landing. Thus, the trajectories investigated here are viewed as potential TransHab technology demonstrators for an eventual crewed Mars mission.[4,8–10] Trajectories beyond 31 December 2011 are not considered because it is assumed that a TransHab flyby mission must be initiated by this date if data from the crew and spacecraft performance are to be incorporated into the operations and hardware of a Mars landing mission as early as 2018.

Trajectory Model

The hybrid optimizer operates on a simple trajectory model composed of two parts, as shown in Fig. 1. The first component is the trajectory module, which computes raw data [such as time of flight

Received 13 September 1999; revision received 1 March 2000; accepted for publication 21 March 2000.

*Graduate Student, Center for Space Research. Member AIAA.
†Associate Professor, Center for Space Research. Associate Fellow AIAA.
‡Professor, Center for Space Research. Fellow AIAA.
§Orbit Analyst, Satellite Network Operations Center, 44330 Woodridge Parkway.

Table 1 Trajectory sequence events

Event	Description	Sequence parameters	Optimization parameters
Departure	Start of trajectory	Start body	Event time
Arrival	End of trajectory	Event number, end body	Event time
Encounter	Unpowered gravity assist flyby	Event number, flyby body	Event time
PFM	Powered gravity assist flyby	Event number, PFM body	Event time
DSM	Impulsive deep space maneuver	Event number	Event time, DSM location (x, y, z)

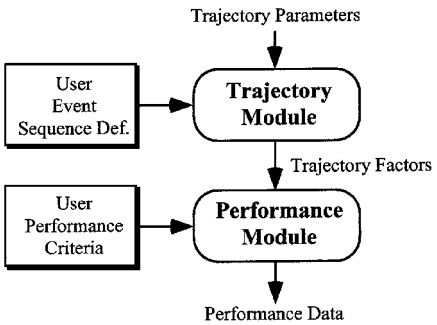

Fig. 1 Hybrid optimizer trajectory model.

(TOF) and ΔV] from parameters such as mission event times and maneuver locations. The second component of the model, the performance module, is tasked with converting the resulting trajectory data into quantities to indicate trajectory parameter set performance. The trajectory model is invoked for each set of trajectory parameters considered by the optimization routines of the hybrid optimizer. The trajectory module processes trajectories utilizing two-body equations of motion, Lambert targeting, and patched conic analysis[11,12] to provide a design-level gravity-assist trajectory model that is simple to use and computationally nonintensive.

To utilize the hybrid optimizer, the mission designer first builds a trajectory based on a sequence of events selected from Table 1. Each event in this sequence contains a time parameter that is manipulated within the optimization process. Though the event sequence remains unchanged, manipulation of event timing provides different candidate trajectories over the course of optimization. As a special case, the deep space maneuver (DSM) event contains additional location parameters which can be manipulated by the optimizer.

The performance module quantifies trajectory performance via trajectory factors and user-selected performance criteria. Trajectory factors are properties of a given trajectory and include quantities such as TOF, ΔV, departure energy, and flyby radius. The mission designer selects from these factors to assemble performance criteria to be optimized or constrained. The performance criteria available to the hybrid optimizer are listed as follows. The performance functions are 1) departure energy, 2) velocity change for orbit departure, 3) arrival energy, 4) velocity change for orbit injection at arrival, 5) velocity change for a powered flyby maneuver (PFM), and 6) velocity change for a DSM. The equality constraints are 1) unpowered flyby (V_∞ matching) and 2) time critical (fixed time parameter). The inequality constraints are 1) planetary flyby radii (minimum), 2) event time parameter window (minimum), 3) event time parameter window (maximum), 4) TOF (maximum), 5) event time ordering, and 6) arrival V_∞ (maximum).

According to the specific needs of the mission designer, selected performance criteria are weighted and applied to candidate trajectories in the form of a scalar performance index function, equality constraint functions, and inequality constraint functions. Evaluations of these functions are made directly available to the GA and RQP components of the hybrid optimizer, which attempts to find an optimum solution for the trajectory in terms of these functions.

The TransHab mission profile was defined by sequencing an Earth departure, a Venus or Mars PFM, and a returning Earth arrival as provided in Table 1. The impulse to initiate transplanetary insertion

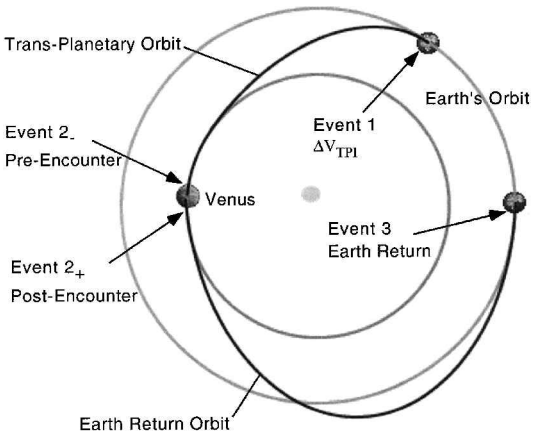

Fig. 2 Mission profile illustration (EVE).

(TPI) is assumed to occur from a 400-km altitude circular orbit from Earth, and the Earth return mode is left undetermined to allow for aerocapture and propulsion options. A qualitative illustration of a representative EVE mission defined by $\boldsymbol{T}$ is shown in Fig. 2. A particular flyby mission is defined in the GA via the timing parameter set

$$\boldsymbol{T} = \begin{bmatrix} t_{0-1} \\ t_{1-2} \\ t_{1-3} \end{bmatrix} \tag{1}$$

where t_{0-1} is the Earth departure TPI time relative to 1 January of a given year from 2002 to 2011, t_{1-2} is the TOF to Venus or Mars PFM, and t_{1-3} is the total mission TOF from Earth departure to Earth return. The MGRAV component differs from the GA in its timing parameter definition by using times for each event relative to some common epoch date. The practical effects of this difference are that MGRAV timing solutions can be obtained outside the boundaries of GA parameter encoding and that event ordering inequality constraints have to be used in MGRAV to ensure that the flyby occurs between Earth departure and return. For simplicity, the relative timing parameter format in Eq. (1) will be used throughout this discussion.

Hybrid GA/RQP Optimizer

The GA and RQP optimizers have complimentary optimization characteristics, and their combined use forms a single optimization tool superior to each of its individual components. Indeed, when each of these optimizers were used independently on the trajectory model, their capabilities and limitations became evident. The standalone RQP optimizer was consistently able to resolve precise local minima of the trajectory solution spaces, but it was extremely sensitive to the initial optimization parameter set. Slight variations in the initial parameter set used by MGRAV were prone to produce significantly different final solutions that often did not meet all of the mission constraints. It was found that a certain a priori knowledge of the parameter space was needed to reach solutions that were feasible in that all of the constraints were satisfied. The cause of this behavior is that RQP methods search only in directions that minimize performance and tend to operate within performance valleys. Therefore, MGRAV is prone to overlook minima that lie in local valleys not encountered in the process of modifying the initial parameter set. This drawback was quickly found to be limiting because the trajectory solution space for EME missions was found to be highly constrained. On the other hand, the GA operates by comparing candidate parameter sets in initially disjoint regions of the parameter space. The GA utilized here is a binary chromosome implementation that maps the real-valued timing parameters from binary chromosome arrays of finite length, implying a finite precision in the resolution of timing parameters. Performance is interpreted as reproduction probability that is used to recombine information contained in the chromosomes into successive generations of comparative solutions in a survival-of-the-fittest analog.

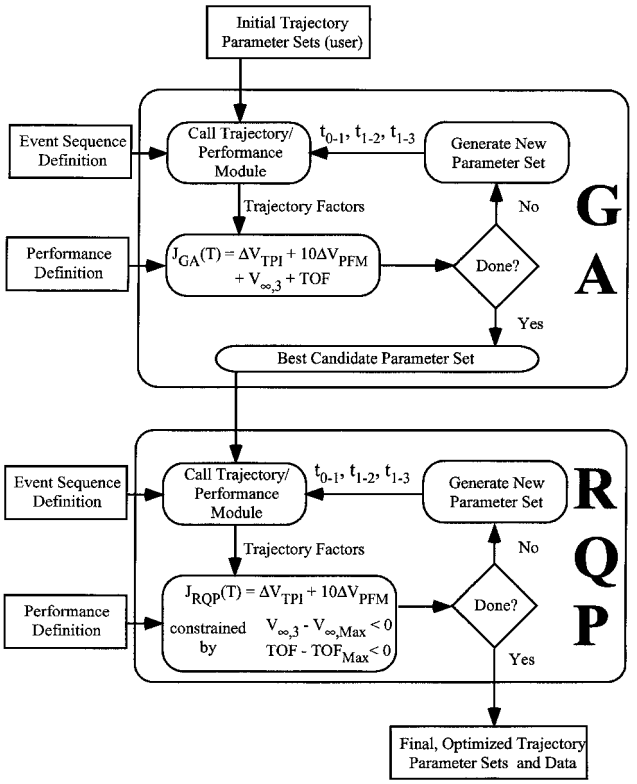

Fig. 3 Hybrid optimizer.

This approach makes the GA resistant to initial poor parameter selection, but causes difficulty in differentiating between solutions once the population has converged to a region of high performance where the GA begins to evenly distribute reproduction probability among population members.

The hybrid optimizer uses a sequential application of the GA and RQP methods on the trajectory model, as shown in Fig. 3. In essence, the GA serves a starter engine that identifies regions of global minima within the trajectory solution space that the RQP approach can then refine to pinpoint the minimum parameter solution with fine resolution. The GA and RQP routines input the trajectory timing parameters into the trajectory model and make changes to the parameter sets based on the output from the performance module. Once the GA has reached a specified number of generations, the candidate trajectory solution with the best performance is submitted to the RQP engine in MGRAV for fine tuning. Elitism is employed in the GA to ensure that the best candidate solution is retained throughout the genetic process.[13] The reader is encouraged to consult the literature for more information on the application and implementation of GAs or the numerical optimization literature for more information on RQP methods.[13–18]

Overview of Hybrid Performance Implementation

The performance indices for the GA and MGRAV modules were constructed from the criteria outlined earlier. One feature of the hybrid optimizer is that slightly different performance definitions may be used by the GA and RQP modules. Both modules utilized ΔV_{TPI}, ΔV_{PFM}, $V_{\infty,3}$, and TOF as performance criteria, but the GA included all of these factors in the single unconstrained performance whereas MGRAV optimized the weighted sum of ΔV_{TPI} and ΔV_{PFM} constrained by inequality conditions on $V_{\infty,3}$ and TOF. The GA performance index is specifically given by

$$J_{GA}(\boldsymbol{T}) = w_{TPI}\Delta V_{TPI} + w_{PFM}\Delta V_{PFM} + w_{V_{\infty,3}} V_{\infty,3} + w_{TOF}\text{TOF} \quad (2)$$

where the weights before the performance criteria represent user-selected values to be discussed hereafter. The effect of this performance definition is that the GA seeks to minimize the weighted sum of all mission values of interest without constraints. This approach was chosen to allow the GA to seek trajectories favorable in all criteria without prematurely excluding missions that may have genetic information of use to the remaining population of solutions. As TOF is typically two orders of magnitude larger than the other performance criteria, the GA tended to produce final results that sacrificed mission ΔV for the sake of lower TOF. Once the GA considered the specified number of solutions, the MGRAV tool then modified the best GA solution by placing inequality constraints on $V_{\infty,3}$ and TOF while minimizing

$$J_{MGRAV}(\boldsymbol{T}) = w_{TPI}\Delta V_{TPI} + w_{PFM}\Delta V_{PFM} \quad (3)$$

The constraints on $V_{\infty,3}$ and TOF are applied according to the active set method so that they do not affect the MGRAV performance in Eq. (3) if they are satisfied. These constraints were chosen to be 14 km/s for $V_{\infty,3}$ and 480 days for TOF. Realistic constraints for TOF are highly dependent on TransHab life support and maintenance specifics, and so 480 days was arbitrarily chosen because it is longer than most low-Earth-orbit (LEO) crewed missions and approximately half the duration of potential three-year Mars exploration missions. The $V_{\infty,3}$ constraint of 14 km/s is relaxed from the roughly 9 km/s suggested by Munk[19] to allow the optimizer to survey a parameter space including trajectories slightly more energetic at than desired Earth return. The utilization of two performance formulations allowed the hybrid optimizer to locate a parameter region initially that was likely to satisfy the $V_{\infty,3}$ and TOF constraints and then to refine the search in this region to optimize only the critical factors of mission ΔV.

GA Implementation

The GA implementation utilizes the following performance evaluation:

$$J_{GA}(\boldsymbol{T}) = \boldsymbol{W}_{GA}^{T}\boldsymbol{O}(\boldsymbol{T}) \quad (4)$$

where

$$\boldsymbol{O}(\boldsymbol{T}) = [\Delta V_{TPI} \quad \Delta V_{PFM} \quad V_{\infty,3} \quad \text{TOF}]^{T} \quad (5)$$

$$\boldsymbol{W}_{GA} = \left[w_{TPI} \quad w_{PFM} \quad w_{V_{\infty,3}} \quad w_{TOF}\right]^{T} \quad (6)$$

Thus, the GA seeks timing parameter sets $\boldsymbol{T}$ that minimize the weighted sum of mission ΔV, $V_{\infty,3}$, and TOF. The specific $\boldsymbol{W}_{GA}$ used by the optimizer was

$$\boldsymbol{W}_{GA} = [1 \quad 10 \quad 1 \quad 1]^{T} \quad (7)$$

where additional weight has been placed on the ΔV_{PFM} magnitude to discourage large maneuvers at the flyby encounter. This approach is reasonable given the nature of the rocket equation

$$\Delta V = c\,\ell n[m_0/(m_0 - \Delta m)] \quad (8)$$

which requires than an exponential quantity of fuel, Δm, be expended at exhaust velocity c to achieve a desired ΔV on the initial total spacecraft mass m_0. A simple staging analysis assuming nominal exhaust velocities will demonstrate that ΔV_{PFM} magnitudes of a few hundred meters per second can prohibitively increase the amount of mass that must be accelerated from Earth orbit to execute the flyby mission.[20] The GA that minimizes Eq. (4) will seek a solution in the region of the parameter space with desirable mission qualities and appropriately emphasizes the high cost of midmission fuel requirements.

The timing parameters were encoded in binary chromosomes according to Table 2, allowing the GA to resolve the solution space to better than 1-day precision.[13] A single trajectory solution is defined by a 25-bit chromosome at this precision level, allowing for

Table 2 GA timing parameter chromosome encoding

Parameter	Minimum, day	Maximum, day	Bit length	Precision, day
t_{0-1}	0	365	9	0.7143
t_{1-2}	80	280	8	0.7843
t_{1-3}	281	481	8	0.7843

2^{25} possible parameter set realizations. The rule of thumb for this particular GA implementation has been to use a population size and number of generations at least equivalent to the total bit length of the chromosome.[21] Therefore, the GA was set to execute 40 generations of 30 population members each to canvas loosely the parameter space with a total of 1200 trajectory evaluations. If needed, a larger population size could be used to perform a more thorough search of the parameter space. Note that the GA has an implicit TOF constraint built into the parameter mapping in that it will only consider solutions within these chromosome boundaries. The RQP optimizer in MGRAV will require penalty functions to enforce event ordering as well as the Earth departure to Earth return TOF constraint.

RQP Implementation

The performance index for the RQP optimization problem was represented as

$$J(\boldsymbol{T}) = \phi(t_{0-1}, t_{1-2}, t_{1-3}) \tag{9}$$

subject to the inequality constraints

$$\Theta(t_{0-1}, t_{1-2}, t_{1-3}) \leq 0 \tag{10}$$

where the objective function ϕ is defined as

$$\phi(t_{0-1}, t_{1-2}, t_{1-3}) = \boldsymbol{W}_O^T \Delta \boldsymbol{V} \tag{11}$$

$\boldsymbol{W}_O$ is an objective weighting vector, and ΔV is the vector of impulsive maneuver magnitudes. The flyby mission plan defines the quantities $\boldsymbol{W}_O$ and ΔV as

$$\Delta \boldsymbol{V} = \begin{pmatrix} \Delta V_{\text{TPI}} \\ \Delta V_{\text{PFM}} \end{pmatrix} \qquad \boldsymbol{W}_O = \begin{pmatrix} w_{\text{TPI}} \\ w_{\text{PFM}} \end{pmatrix} \tag{12}$$

where $w_{\text{TPI}}, w_{\text{PFM}} > 0$.

The constraint function implemented in MGRAV also assigns weights to each constraint element

$$\Theta(t_{0-1}, t_{1-2}, t_{1-3}) = \boldsymbol{W}_C^T \boldsymbol{C} \leq 0 \tag{13}$$

where $\boldsymbol{W}_C$ is the vector of constraint weights and $\boldsymbol{C}$ is the vector of constrained elements. This constraint vector is defined as

$$\boldsymbol{C}(t_{0-1}, t_{1-2}, t_{1-3}) = \begin{bmatrix} V_{\infty,3} - V_{\infty,\max} \\ \text{TOF} - \text{TOF}_{\max} \\ \boldsymbol{\Theta}_{\text{mission}} \end{bmatrix} \tag{14}$$

where the partition $\boldsymbol{\Theta}_{\text{mission}}$ is an operational constraint vector utilized by the MGRAV code to ensure compliance with the mission design. Specifically, the MGRAV operational constraints require proper event ordering ($t_1 < t_2 < t_3$) and mission feasibility (flyby radius above planetary atmosphere $r_{\text{PFM}} > r_{\text{target}}$). As already discussed, the constraint quantities were chosen to be 480 days for $\text{TOF}_{\max}$ and 14 km/s for $V_{\infty,\max}$.

The total weight vector for MGRAV operation is thus

$$\boldsymbol{W}_{\text{MGRAV}} = [\boldsymbol{W}_O \quad \boldsymbol{W}_C]^T \tag{15}$$

This vector is a notational convenience because it contains weights for constructing the relative importance of the optimized and constrained performance criteria. The specific values used in the results presented here were

$$\boldsymbol{W}_{\text{MGRAV}} = [1 \quad 10 \quad 1 \quad 1 \quad 1+]^T \tag{16}$$

where the 1+ indicates unity weighting for all necessary MGRAV operational constraints.[7] The constraint methodology in MGRAV employs the active set approach so that operational constraints, Earth arrival speed, and TOF will not affect the performance index if they are below their respective inequality thresholds.

Results

Mission Performance

The mission ΔV, $V_{\infty,3}$, and TOF values from the EME and EVE hybrid optimization iterations are listed in Table 3. Note that trans-planetary insertions are distinguished by trans-Venus insertion (TVI) and trans-Mars insertion (TMI) labels for the appropriate target. By assuming that 5 km/s is a reasonable limiting value for ΔV_{TPI} in LEO, one EME and five EVE missions were found with acceptable propulsion requirements. Furthermore, all but one of the EVE missions required a LEO impulse of less than 10 km/s, whereas only five of EME missions were below this value. As an interesting historic perspective, the requirement for trans-lunar insertion ΔV during the Apollo exploration program was about 3.5 km/s. The utility of the increased optimization weight placed on the PFM is evident because the majority of EVE and EME ΔV_{PFM} magnitude requirements are less than 1 km/s. Half of the EME results presented here were unable to meet the $V_{\infty,3}$ constraint of 14 km/s, due in large part to the 480-day TOF limitation. Higher TOF constraints allow for EME missions with less energetic Earth return modes. The significance of the 480-day TOF constraint on the EME mission design is that larger population sizes should be used to isolate any narrow regions in the parameter space that might just barely conform to the mission constraint requirements.

Table 3 Mission ΔV results 2002–2011

	EVE				EME			
Year	ΔV_{TVI}, km/s	ΔV_{PFM}, km/s	$V_{\infty,3}$, km/s	TOF, day	ΔV_{TMI}, km/s	ΔV_{PFM}, km/s	$V_{\infty,3}$, km/s	TOF, day
2002	3.5279	0.0058	7.2925	384	8.6836	0.1254	11.7478	359
2003	5.3154	0.3974	5.5826	433	4.0119	1.6705	11.7652	470
2004	3.7447	0.0384	8.1435	373	9.3590	0.2898	13.2250	368
2005	5.0462	0.7721	8.5258	374	14.838	2.1455	23.8192[a]	383
2006	6.4575	0.1033	13.334	313	9.0729	0.0141	12.0645	354
2007	3.6824	0.0202	7.7346	377	6.8514	1.0146	16.6848[a]	481
2008	5.5044	0.0881	3.5482	374	11.309	0.9260	18.8728[a]	364
2009	4.9280	0.9120	8.2613	335	12.642	0.5674	18.8920[a]	363
2010	3.5194	0.0134	7.3384	389	13.000	0.18252	18.3185[a]	354
2011	5.7284	0.1338	3.4192	365	13.798	1.3732	14.000	377

[a]Failure to meet constraints.

Table 4 Best solutions for EVE missions

Parameter	2002 launch	2004 launch	2007 launch	2010 launch
t_{0-1}, day	217.2823	82.2691	149.4338	214.1381
t_{1-2}, day	121.6105	114.2393	116.7257	122.6202
t_{1-3}, day	384.7392	373.2496	377.4699	389.2965
ΔV_{TVI}, km/s	3.5279	3.7447	3.6824	3.5194
ΔV_{PFM}, km/s	0.0058	0.0384	0.0202	0.0134
$V_{\infty,3}$, km/s	7.2341	8.1435	7.7346	7.3384
δ_{Venus}, deg	60.9355	70.1135	75.5107	56.7916
δ_{sun}, deg	7.2994	8.6743	7.7344	6.6674
Flyby radius, km	12,167.5	8,816.4	10,536.1	14,217.9
Flyby altitude, km	6,116.5	2,765.4	4,485.1	8,166.9
Lambert calls: GA	2,400	2,400	2,400	2,400
Lambert calls: MGRAV	152	152	280	152

Table 5 Best solutions for EME missions

Parameter	2002 launch	2003 launch	2004 launch	2006 launch
t_{0-1}, day	244.3152	113.3458	270.6252	380.8780
t_{1-2}, day	270.1730	187.2066	222.3118	226.2744
t_{1-3}, day	358.6353	469.9329	368.1226	353.5815
ΔV_{TMI}, km/s	8.6836	4.0119	9.3590	9.0728
ΔV_{PFM}, km/s	0.1254	1.6705	0.2898	0.0144
$V_{\infty,3}$, km/s	11.7479	11.7653	13.2251	12.0645
δ_{Mars}, deg	25.9156	38.8287	3.4922	26.2177
δ_{sun}, deg	7.8596	5.1076	1.7590	8.4921
Flyby radius, km	3,596.9	3,596.9	19,136	3,596.3
Flyby altitude, km	203.6	203.6	15,743	202.9
Lambert calls: GA	2,400	2,400	2,400	2,400
Lambert calls: MGRAV	238	504	56	476

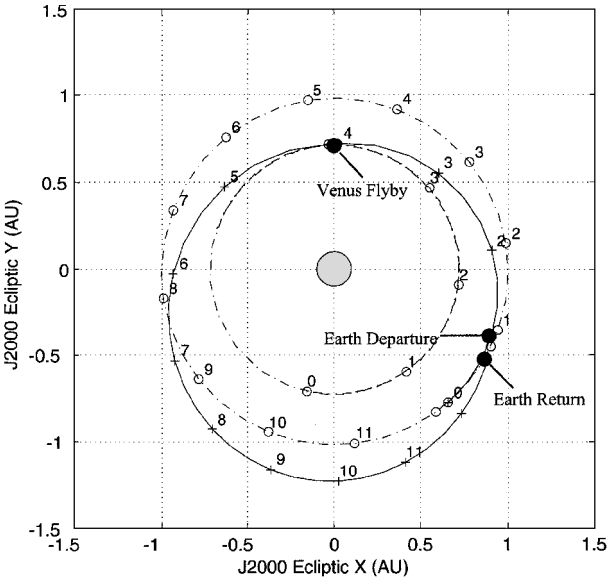

Fig. 4 EVE trajectory for 2010 (planar projection).

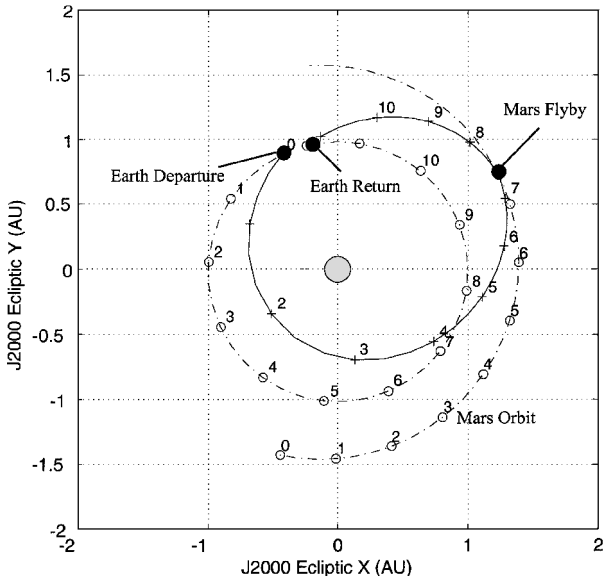

Fig. 5 EME trajectory for 2006 (planar projection).

The full performance criteria for the most promising hybrid optimizer results can be found in Tables 4 and 5, which include the trajectory timing parameters, the mission ΔV, the trajectory turn performed by the powered flyby, the flyby altitude, and the number of Lambert evaluations needed by each of the optimization modules. This collection of missions assumes that $\Delta V_{\mathrm{TPI}} = 10$ km/s is the limiting magnitude for both missions. Of particular interest are the EVE 2002, EVE 2010, EME 2002, and EME 2006 missions, which offer the best performance indices of the missions provided. The trajectories of the EVE 2010 and the EME 2006 missions can be viewed in Figs. 4 and 5, with the planar projection of the positions of Earth and Venus or Mars displayed at 30-day intervals. Figures 6–9 show contours of EVE 2010 and EME 2006 missions for ΔV_{TPI} and $V_{\infty,3}$.

To corroborate the optimality of these results, a three-dimensional grid search was performed with 5-day time steps over each timing parameter covering the span indicated in Table 2. The results from this verification are provided in Table 6 for the EVE 2002, EVE 2010, EME 2002, and EME 2006 departure missions. These timing vector parameters are compared to the results from the hybrid optimizer in a graphical format in Figs. 6 and 9, where the results from the GA and MGRAV modules of the hybrid optimizer are plotted along

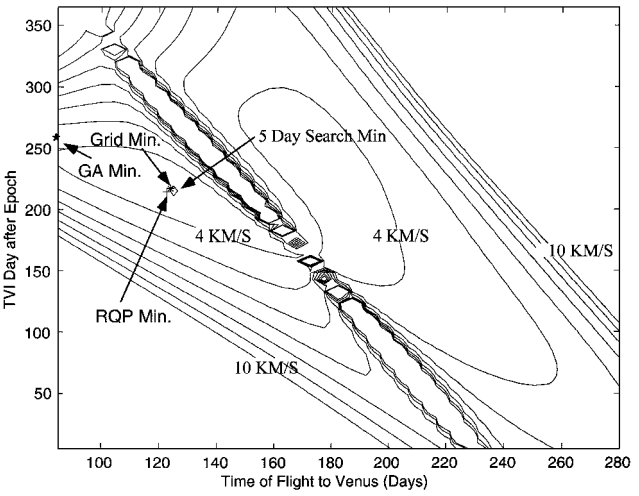

Fig. 6 EVE 2010 ΔV_{TPI} contours.

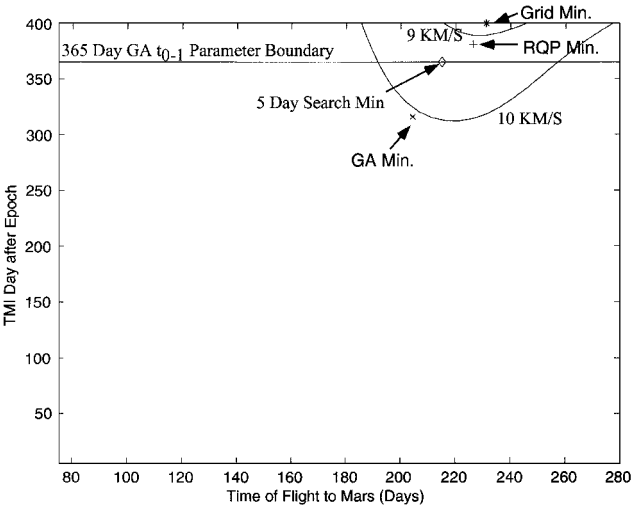

Fig. 7 EME 2006 ΔV_{TPI} contours.

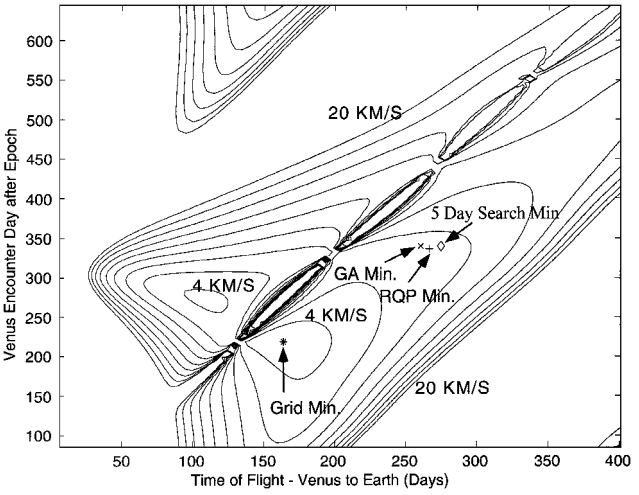

Fig. 8 EVE 2010 $V_{\infty,3}$ contours.

with the 5-day grid search results against the backdrop of ΔV_{TPI} and ΔV_{PFM} pork chop contours.

The hybrid encounter times are all located near 5-day grid search results and perform on a par with the results of the grid search in terms of Eq. (11). However, inspection of the TOF for the EVE missions indicate that the MGRAV search remained in the valley of the GA module's best performing parameters, which included TOF in the performance index 4. The 5-day grid search required 248,788

Table 6 Best grid search solutions for EME and EVE missions

Parameter	Flyby planet			
	Venus, 2002 launch	Venus, 2010 launch	Mars, 2002 launch	Mars, 2006 launch
t_{0-1}, day	215	215	240	365
t_{1-2}, day	120	125	265	215
t_{1-3}, day	411	401	356	356
ΔV_{TPI}, km/s	3.5341	3.5338	8.8814	9.2709
ΔV_{PFM}, km/s	0.0026	0.0021	0.0056	0.0140
$V_{\infty,3}$, km/s	7.8491	7.5439	12.7321	13.2162
δ_{target}, deg	29.9306	44.5591	22.6110	10.5014
δ_{sun}, deg	3.0266	4.9955	7.6558	3.4680
Flyby radius, km	32,514	21,582	4,039.9	8,541.3
Flyby altitude, km	26,463	15,531	646.5	5,147.9
Lambert calls	248,788	248,788	248,788	248,788

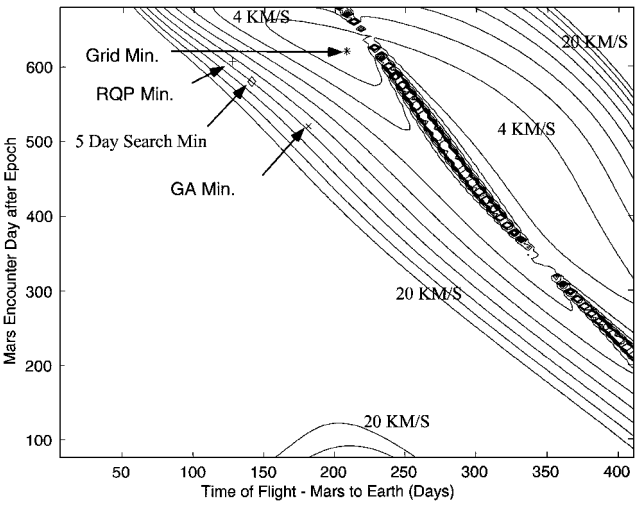

Fig. 9 EME 2006 $V_{\infty,3}$ contours.

Lambert evaluations per mission, a value two orders of magnitude greater than required by the average hybrid optimization run.

Hybrid Optimizer Operation

The hybrid optimizer was found to generally create acceptable solutions without requiring a priori knowledge of feasible timing parameter sets. However, the small population size utilized by the GA resulted in a sensitivity to the seed value used to initialize its random number generator. Because the hybrid optimizer utilized a serial union of the GA and MGRAV engines, this sensitivity propagated to the final MGRAV parameter solution. Optimizing EME solutions that satisfied all of the inequality constraints proved difficult as the 480-TOF limit highly constrained the parameter space. Additionally, because the GA solution only sought to minimize the sum of trajectory factors, it is not guaranteed to present MGRAV with an initial parameter set in a region of the parameter space that could be refined to a feasible solution. The EVE mission solutions were sufficiently within the mission constraints that the hybrid optimizer was easily able to create feasible solutions and did not display a significant sensitivity to GA random seed initialization. Experimentation with larger population and generation sizes in the GA indicate that several EME solutions satisfying TOF and $V_{\infty,3}$ constraints are available, but at the cost of prohibitive mission ΔV.

Conclusions

The hybrid optimizer was created to utilize the strengths of the GA and RQP optimization techniques. The GA acts as a startup engine to search the parameter space for regions of global extrema. The best solution from the GA is then used by the RQP engine as an initial guess in a calculus-based RQP optimization. Based on an evaluation of prospective TransHab missions, the hybrid optimizer was shown to exhibit performance on par with a standard grid-type parameter search with two orders of magnitude fewer trajectory evaluations. This improved efficiency would allow the mission designer the flexibility to consider several different event sequences and performance definitions in a feasibility study. In particular, a mission designer could quickly determine how much the TOF constraint needed to be relaxed to allow for a greater selection of EME trajectories. The results of the TransHab mission analysis indicate that Venus is a superior target to Mars for TOF and return energy constrained flyby missions in terms of mission ΔV and mission opportunities. The recurrence of EVE solutions is consistent with the 1.6-year synodic period and 8-year inertial period of the Earth–Venus system, but the entire 15-year Earth–Mars inertial cycle was not covered because of the mission cutoff date for incorporation of results into a human Mars landing mission as early as 2018. The most promising EVE missions required ΔV on par with lunar missions and had negligible PFM requirements at Venus. In the current serial implementation, the hybrid optimizer uses the best GA solution to provide a likely starting parameter set for MGRAV. The hybrid optimizer might be improved by altering this structure to a parallel implementation, where each population member of the GA is used as an initial parameter set for a RQP search. The performance from each RQP search within the population would then be used as the performance for the respective population member in the GA. In this manner, the GA would consider the space of potential starting parameter sets by evaluating each set's final performance after RQP refinement. This approach could greatly assist in searching for trajectories in highly constrained parameter spaces such as encountered in the EME missions investigated here.

Acknowledgments

This work was supported in part by a Graduate Research Fellowship Grant from the National Science Foundation. Special thanks are due to Bedford Cockrell at NASA Johnson Space Center for suggesting the TransHab problem to us and for his helpful discussions.

References

[1]Striepe, S. A., and Braun, R .D., "Effects of a Venus Swingby Periapsis Burn During an Earth–Mars Trajectory," American Astronautical Society, Paper 89-426, Aug. 1989.

[2]Gillespie, R. W., and Ross, S., "Venus-Swingby Mission Mode and Its Role in the Manned Exploration of Mars," *Journal of Spacecraft*, Vol. 4, No. 2, 1967, pp. 170–175.

[3]Ordway, F. I., "Mars Mission Concepts: The Von Braun Era," *Strategies for Mars: A Guide to Human Exploration*, edited by C. R. Stoker and C. Emmart, Vol. 86, Science and Technology Series, American Astronautical Society, San Diego, CA, 1996, pp. 68–96.

[4]Niehoff, J. C., and Hoffman, S. J., "Pathways to Mars: An Overview of Flight Profiles and Staging Options for Mars Missions,"*Strategies for Mars: A Guide to Human Exploration*, edited by C. R. Stoker and C. Emmart, Vol. 86, Science and Technology Series, American Astronautical Society, San Diego, CA, 1996, pp. 98–125.

[5]D'Amario, L. A., Bright, L. E., and Wolf, A., "Galileo Trajectory Design," *Space Science Reviews*, Vol. 60, No. 1–4, 1992, pp. 23–78.

[6]Chaer, W. S., and Bishop, R. H., "Adaptive Kalman Filtering with Genetic Algorithms," American Astronautical Society, Paper 95-143, Feb. 1995.

[7]Rock, K. M., "A Design Tool for the Optimization of Multiple Body Gravity Assist Trajectories," M.S. Thesis, Dept. of Aerospace Engineering and Engineering Mechanics, Univ. of Texas, Austin, TX, Dec. 1996.

[8]Griffin, M. D., "Managing the Exploration of the Moon and Mars," *Strategies for Mars: A Guide to Human Exploration*, edited by C. R. Stoker and C. Emmart, Vol. 86, Science and Technology Series, American Astronautical Society, San Diego, CA, 1996, pp. 59–66.

[9]Lee, V. A., and Wilson, S. A., "A Survey of Ballistic Mars-Mission Profiles," *Journal of Spacecraft and Rockets*, Vol. 4, No. 2, 1967, pp. 129–142.

[10]Finney, B., "From the Great Voyages of Exploration to Missions to Mars," *Strategies for Mars: A Guide to Human Exploration*, edited by C. R. Stoker and C. Emmart, Vol. 86, Science and Technology Series, American Astronautical Society, San Diego, CA, 1996, pp. 268–282.

[11]Bate, R. R., Mueller, D. D., and White, J. E., *Fundamentals of Astrodynamics*, 1st ed., Dover, New York, 1971, pp. 228–271, 359–380.

[12]*Astronomical Almanac*, U.S. Naval Observatory, Washington, DC, 1996, p. E3.

[13]Goldberg, D. E., *Genetic Algorithms in Search, Optimization, and Machine Learning*, 1st ed., Addison Wesley Longman, Reading, MA, 1989, p. 115.

[14]Ladd, S. R., *Genetic Algorithms in C++*, 1st ed., M&T Books, New York, 1996, pp. 61–106.

[15]Ely, T. A., Crossley, W. A., and Williams, E. A., "Satellite Constellation Design for Zonal Coverage Using Genetic Algorithms," American Astronautical Society, Paper 98-128, Feb. 1998.

[16]Mahfoud, S. W., "Population Size and Genetic Drift in Fitness Sharing," *Foundations of Genetic Algorithms*, Morgan Kaufmann, San Francisco, 1995, pp. 185–223.

[17]Hartmann, J. H., Coverstone-Carroll, V., and Williams, S. N., "Optimal Interplanetary Spacecraft Trajectories Via a Pareto Genetic Algorithm," American Astronautical Society, Paper 98-202, Feb. 1998.

[18]Casalino, L., Colasurdo, G., and Pastrone, D., "Optimization Procedure for Preliminary Design of Opposition-Class Mars Missions," *Journal of Guidance, Control, and Dynamics*, Vol. 21, No. 1, 1998, pp. 134–140.

[19]Munk, M. M., "Departure Energies, Trip Times and Entry Speeds for Human Mars Missions," American Astronautical Society, Paper 99-103, Feb. 1999.

[20]Crain, T. P., "Application of a Hybrid Optimizer to a Mission Design for Mars Transhab Verification," M.S. Thesis, Dept. of Aerospace Engineering and Engineering Mechanics, Univ. of Texas, Austin, TX, May 1999.

[21]Fowler, W. T., Crain, T. P., and Eisenreich, J., "The Influence of Coordinate System Selection on Genetic Algorithm Optimization of Low-Thrust Spacecraft Trajectories," American Astronautical Society, Paper 99-130, Feb. 1999.

C. A. Kluever
Associate Editor